university of groningen / faculty of science and engineering / biomedical engineering

Optimization of pushrim-activated power assisted wheelchair structure to prevent tipping injuries

Johan Hoksbergen
S4973267

Biomedical Engineering (Medical Device Design)
Faculty of science and engineering, Engineering and Technology Institute Groningen (ENTEG), University of Groningen

Groningen, May 2024 - June 2024

Bachelor's project

Supervisor (first examiner): Dr. E. Wilhelm, assistant professor, ENTEG

Second examiner: Dr. Ir. C. Roossien, ENTEG

ENTEG Engineering and Technology institute Groningen

Abstract

The introduction of a pushrim activated power assisted wheelchair allows for users with some extent of functional use of upper extremities to propel themselves and thereby reduce muscular atrophy. However, wheelchair tipping injuries remain a safety concern for users, particularly those navigating uneven terrains or slopes.

In this thesis, the design and optimization of a pushrim-activated power assisted wheelchair (PAPAW) is presented, aimed at reducing dynamic tipping probability. A small scale model PAPAW (3.5 : 1) was constructed to determine the effect of different design parameters on tipping behavior. These parameters, yielding 4 prototypes, included a modification of wheelchair dimensions, battery placement, introduction of a weighted base structure and the addition of anti tipping wheels. These prototypes were tested for static tipping angles and dynamic stability driving down curbs of 50 mm and 70mm heights, approaching the curbs at 30°, 60° and 90° angles.

The results demonstrated that anti-tipping wheels significantly enhanced rear stability, while a heavier bottom base (lower center of gravity) improved front stability, which complies with previous studies done by Kirby R.L. (1996) and Thomas L. et al (2018) respectively. However, minor alterations in dimensions as well as battery placement did not record a measurable difference in tipping probability. Thus, this thesis concludes that the combination of anti tipping wheels and a lower center of mass can substantially mitigate tipping risks, offering a safer and more reliable mobility solution for power assisted wheelchair users.

Table of Contents

1. Introduction

Wheelchairs are a type of assistive technology that are important as they facilitate the active engagement of users in everyday activities, reducing the psychological impact of their limited mobility [1]. According to the WHO roughly 65 million people currently use both powered as well as manual wheelchairs [2]. The latter stimulates the users with some extent of functional use of upper extremities to propel themselves and thereby maintain the muscular power they still have and reduce muscular atrophy [3]. However, for many wheelchair users this requires exerting more force than they are physically capable of.

Thus, pushrim-activated power assisted wheelchairs (PAPAW) are currently being developed and optimized. A PAPAW is a type of semi-powered wheelchair that interprets the force applied by the user on the pushrim, amplifies it and converts it into momentum in the wheels [4]. It stimulates maximal muscle usage for wheelchair users with limited physical ability. Even though PAPAWs enhance active maneuverability and muscle mass preservation, they also pose challenges. A study performed by Kamarker et al. (2008) investigated the dynamic stability properties of the current PAPAWs on the market according to the ANSI/RESNA standards. The dynamic stability results from the study indicate that stability decreases as the surface angle increases to 10 degrees. This becomes particularly relevant with outdoor mobility, where users encounter obstacles and uneven terrain, which increases the risk of tipping and the associated injuries [5].

In fact, tipping associated injuries are the most prominent injuries among wheelchair users [6]. From this it can be concluded that current wheelchairs lack sufficient stability and this safety concern is addressed in this thesis by optimizing the wheelchair structure. Many features of wheelchair structure can be changed and optimized to achieve more stability, such as changing the total weight distribution to alter the gravitational center of mass of the wheelchair [7]. However, it is of pivotal importance the requirements and wishes of the wheelchair users must be taken into account during the design process. Consequently the design of a dynamically stable wheelchair faces many challenges and limitations.

In this thesis, the aim is to design a pushrim-activated power assisted wheelchair, specifically engineered to reduce dynamic tipping probability and thereby mitigate the associated tipping injuries.

2. Problem analysis

2.1 Problem definition

In a study done by Wan-Yin Chen et al. (2011) with a sample size of 95 participants including both manual and electric powered wheelchairs, it has been shown that at least 47.59% have reported at least one occurrence of tipping. Approximately 84% of injuries reported in the study were minor injuries and 16% were major injuries such as concussions and fractures [8]. Another study performed in the province of Nova Scotia, Canada (1994) with a sample size of 2055 participants of manual wheelchairs has shown 57.4% accidents involving tips, from which many of the tips occurred outdoors on uneven terrains [9]. These studies demonstrate that the overall tipping mitigation has not yet been significantly reduced as roughly half of all wheelchair users experience tipping accidents, highlighting the importance of further improvements in wheelchair technology. In order to understand the problem it is crucial to understand the mechanism of tipping.

Mechanical analysis of wheelchair tipping

Static tipping occurs when the sum of moments (ΣM) is no longer equal to 0, creating torque [10]. This means the center of gravity (CG) moves past the point of contact (POC) of the wheels with the surface ($\Sigma M \neq 0$). Figure 1 illustrates this principle, where the forces are illustrated with the red arrows.

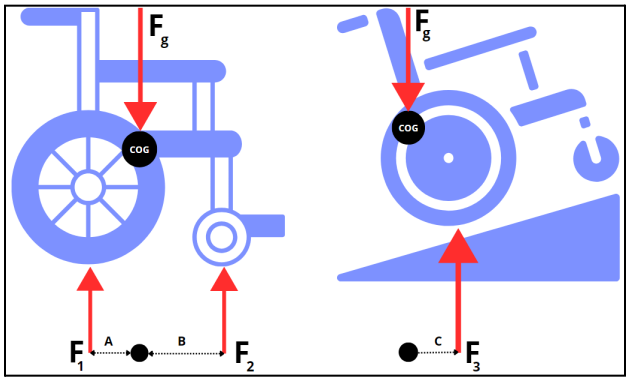

Figure 1: moments on level surface (left) and moment on tilted surface (right).

The forces on the left wheelchair in figure 1 cause an equal and opposite momentum acting on the CG allowing the wheelchair to remain balanced. By injecting the moments from the contact points (M_1 and M_2) in formula 1 and writing the moments as a function of force and distance one obtains formula 2, where A is the horizontal distance from the CG to the rear POC, B is the horizontal distance from the CG to the front POC and F_1 and F_2 the normal forces at the respective POC [10].

$$\Sigma M = 0; \quad (1)$$
$$F_1 A = -F_2 B; \quad (2)$$

Once the angle is increased, the orientation of the wheelchair changes, causing a shift in CG of the wheelchair (right in figure 1). In this case the front wheels lift up off the ground, meaning there is no force acting on the front wheels and the force counteracting the gravitational force is solely dictated by the normal force acting on the rear wheels. By injecting the moment around the point of contact M_3 into formula 1 we obtain formula 3 and the resulting momentum is greater than 0 Nm, which causes the wheelchair to tip over [10]. The same principle applies for lateral tipping.

$$\Sigma M = F_3 C > 0; \quad (3)$$

The angle of the surface that causes tipping is called the tipping angle and is proportional to the height and width of the CG with respect to the POC. The tipping angle is given by formula 4 and can be seen in figure 2 [10][11].

$$\Theta = tan^{-1}(A/B); \quad (4)$$

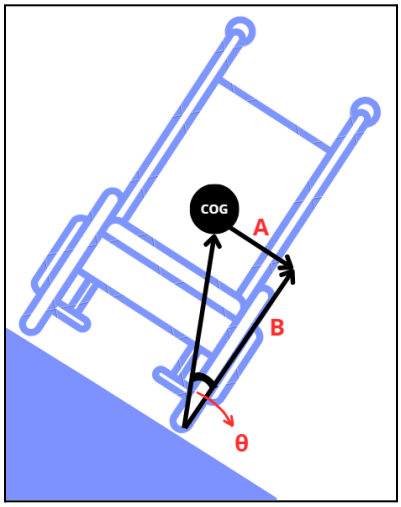

Figure 2: tip angle Θ.

However, dynamic tipping also involves a certain velocity of the wheelchair, which has an effect on the forces acting on the wheelchair. First and foremost linear accelerating and decelerating motion causes a moment about the CG, which is depicted in figure 3. The inertia of the user causes a force (F_q) on the wheelchair during acceleration opposite to the movement direction, whereas deceleration causes the user to move forward in the chair, shifting the center of gravity and thereby changing the moments.

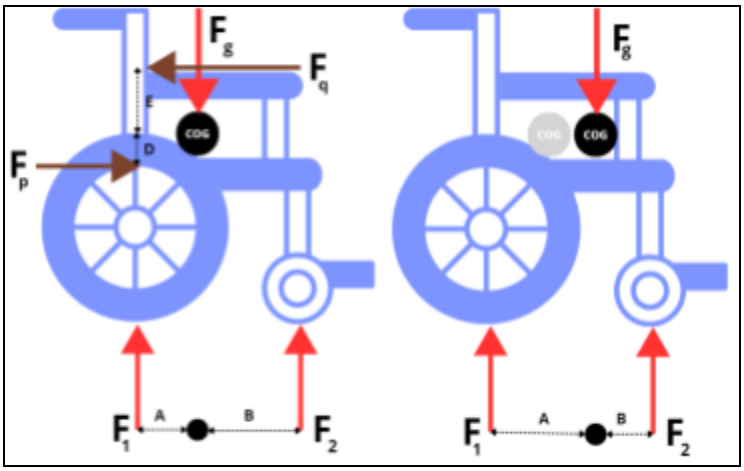

Figure 3: moments caused by linear acceleration (brown arrows) (left) and deceleration by braking (right).

The direction of the moment is dependent on the location of the CG with respect to the hand rims, which is where the propel force (F_p) is being applied. In order to remain balanced and not tip over the moments must be counteracted and results in an increase in normal force F_1. Inserting the moments about the CG into formula 1 gives formula 5, which is the resulting sum of moments [10].

$$F_1 A + F_2 B + F_p D + F_q E = 0; \qquad (5)$$

Lastly, tipping also occurs when a lateral component of acceleration is introduced, causing a centrifugal force to act on the wheelchair. This occurs when a wheelchair makes a turn for instance. When a wheelchair follows a certain circular trajectory with a certain radius (r) then a centrifugal force (F_f) is generated proportional to the radius, mass (m) and velocity (v) of the wheelchair. This can be seen in figure 4, where wheelchair base width is denoted by b and height of CG by h.

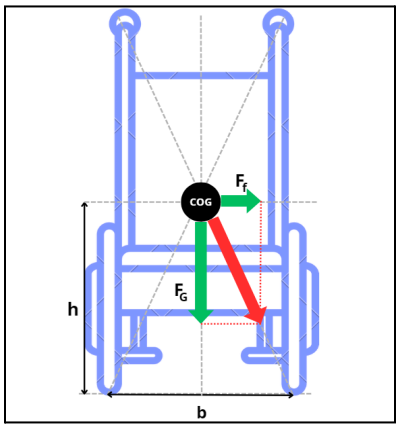

Figure 4: centrifugal force on balanced vehicle [12].

The wheelchair will remain balanced as long as the resultant force (red arrow) does not pass the tilting point. The maximum velocity (v_{max}) a wheelchair can have without tilting is proportional to the location of the center of mass as well as the radius of curvature of trajectory, which is given in formula 6 [12]. Substitution of Centrifugal (7) and gravitational force (8) in formula 6 leads to the derivation of v_{max} and can be seen in formula 9 [12].

$$F_f = F_G * \frac{b}{2h}; \tag{6}$$

$$F_f = \frac{mv^2_{max}}{r}; \tag{7}$$

$$F_G = mg; \tag{8}$$

$$v_{max} = \sqrt{\frac{rbg}{2h}}; \tag{9}$$

Exceeding the maximum velocity will cause a moment M_k around the tilting point as a result of a net horizontal force F_g (yellow arrow) and results in the wheelchair tipping. This can be seen in figure 5.

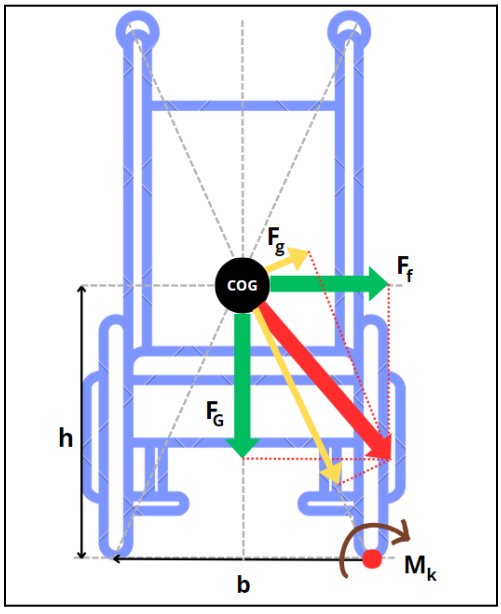

Figure 5: centrifugal force causing vehicle to tip over [12].

In conclusion, the main factors that dictate tipping probability are wheelchair base width, height of CG, mass, velocity and radius of curvature.

2.2 Stakeholders

When optimizing the mechanical features to prevent tipping, the stakeholder requirements and wishes must be taken into account. Stakeholders are an important factor in the design of a PAPAW and table 1 states the stakeholders and their corresponding demands. Stakeholder analysis is essential to be able to provide a solution to the stated problem, because it affects the final outcome such that it successfully serves its purpose.

Table 1: Stakeholder analysis table

stakeholders	characteristics	expectations	Implications and conclusions
Patient	Impaired mobility	Device that enables them to move freely on all terrains without tipping	Device has to achieve movement freedom without risk of tipping
Wheelchair manufacturers	Profit driven	Profit through the introduction of a novel wheelchair (part)	Manufacturing must be profitable
Insurance provider	Care at low cost	Low acquisition costs with effective performance	Device must be cost-effective
Regulatory agencies	Ensure safe device usage	Device complies with standards, guidelines and safety regulations	Device must be safe to use and not cause any harm to patient or the environment
Healthcare professionals	Provide insight into user experience and user needs	Adjustable device to fit needs of all patient	Device has to be adjustable, i.e. One-size-fits-all

2.3 Design assignment

The design assignment is to design a pushrim-activated power assisted wheelchair that fulfills all requirements and wishes from the stakeholders, specifically engineered to reduce static and dynamic tipping probability. It involves the integration of power assistive mechanisms with a traditional manual wheelchair. The main focus lies on developing and improving the wheelchair structure. The wheelchair must be able to assist users that still have power in their upper extremities to be able to propel themselves and fulfill wishes and needs of all stakeholders.

2.4 Market research

The two main PAPAWs currently commercially available are Quickie Extender and Alber E motion. These two designs are most inline with the design assignment proposed in this research. Both designs offer assisted power and can be seen in figure 6.

Figure 6: Alber e-motion PAPAW (left) [13] and Quickie Xtender PAPAW (right) [14].

Some specifications of the PAPAWs can be seen in table 2.

Table 2: specifications of the Xtender and E-motion PAPAW [15].

	Xtender	**E-motion**
Manufacturer	Sunrise medical	Alber
Price	€ 7537	€ 8236
Wheelchair base	Quickie	Quickie
Motor [W]	1 X 150	2 X 150
Battery	24V, 6.7 A/h NiMH	2 X 24V, 6.7 A/h NiMH
Mass [Kg]	59	88
Length ± SD [mm]	1026.57 ± 7.99	1038.75 ± 10.57
Width ± SD [mm]	666.75 ± 27.67	651.93 ± 7.33
Height ± SD [mm]	853.01 ± 1.83	842.43 ± 9.69
Rear wheel diameter [mm]	609.6	609.6
Front wheel diameter [mm]	146.05	146.05

*SD = standard deviation

2.5 Requirements and wishes

2.5.1 Requirements

The design of a PAPAW must meet certain requirements and wishes as stated by the stakeholders. To be able to prioritize and rank all requirements and wishes the Analytical Hierarchy Process (AHP) weighting system was used, which assigns a grade 1-10 based on relative importance to each requirement and wish. The requirements and wishes were formulated and weighted in cooperation with a patient (Impaired mobility in all extremities) and occupational therapist (Nicole Schoeber, Ergodus). The requirements for an improved PAPAW can be seen in table 3. It is important to note a wheelchair frame has personalized seating dimensions, meaning seating width is a distinctive property among users.

Table 3: Requirements for PAPAW

	Description	Weight
Function	1. The wheelchair must provide power assistance when propelled up to 6 $km\ h^{-1}$.	10
	2. The wheelchair must be adjustable.	6
	3. The wheelchair must be easily collapsible to 75% of its original volumetric dimensions by nine out of 10 nurses within 2 minutes, provided a manual and training.	7
	4. The wheelchair must have good maneuverability, meaning the wheelchair must have a maximum turning circle with radius of less than 1250 mm.	9
Safety	1. The wheelchair must not harm the user.	10
	2. The wheelchair must not tip front, rear or lateral side under normal use.	10
Performance	1. The wheelchair must not tip over at speeds less than 6 $km\ h^{-1}$ and a radius of curvature of 1000 mm.	8
	2. The wheelchair, with user and possibly maximum extra weight of 10 kg and sticking out less than 20 cm (e.g. medical equipment or groceries) must not tip over on uneven terrain with a maximum slope of 30 degrees.	8
	3. The battery must last at least 3 hours at max speed on flat surfaces (range ~ 15-18 km).	9
Usage	1. The wheelchair must not require more than 20 N to be propelled by the user itself.	8
Time	1. The lifespan of the product must be at least 7 years, considering normal use, meaning an occupancy time of 11 hours of 10 bouts per hour and 10% wheeling time. [16]	9
	2. The device must only require maintenance, regular checks, repairs and replacements of worn out or damaged parts once a year.	8
Size	1. The wheelchair must not be bigger than 800 x 1000 x 900 mm (WxLxH).	10
	2. The wheelchair frame must not weigh more than 16 kg.	6

2.5.2 Wishes

The wishes for a PAPAW design can be seen in table 4.

Table 4: Wishes for PAPAW

	Description	Weight
Function	1. The wheelchair should provide multiple power assistance magnitudes, i.e. 0%, 25%, 50%, 75% and 100% of maximum output motor. 2. The wheelchair should be collapsible to 50% of the original volumetric dimensions by nine out of 10 nurses within 2 minutes, provided a manual and training. 3. The wheelchair could have a usb port to charge a phone.	4 2 1
Safety	1. The wheelchair should not have any sharp edges or protrusions. 2. The wheelchair could have reflective units.	4 1
Usage	1. The wheelchair should be ergonomic. 2. The wheelchair could have armrests	4 2
Size	1. The wheelchair should not be more visible than 25% of the total frontal view and 60% of the total side view (i.e. see person and not wheelchair) as well as at least 75% of the user must be visible from the side view. 2. The wheelchair should be as lightweight as possible.	5 3
Cost	1. The wheelchair should be as cheap as possible.	5

2.5.3 MoSCoW Method

The requirements and wishes were ordered using the MoSCoW method [17]. This provides an overview of the goals to be achieved for the prototype based on the prioritization weighting (top to bottom). It includes the requirements that must, should, could and won't be met in the design process.

Table 5: MoSCoW Method

	Description
Must have	- The wheelchair must provide power assistance when propelled up to 6 $km\,h^{-1}$. - The wheelchair must not harm the user. - The wheelchair must not tip front, rear or lateral side under normal use. - The wheelchair must not be bigger than 800 x 1000 x 900 mm (WxLxH). - The battery must last at least 3 hours at max speed on flat surfaces (range ~ 15-18 km). - The wheelchair must have good maneuverability, meaning the wheelchair should have a minimal turning circle with radius of ~750 mm. - The lifespan of the product must be at least 7 years, considering normal use, meaning an occupancy time of 11 hours of 10 bouts per hour and 10% wheeling time. - The wheelchair must not tip over at speeds less than 6 $km\,h^{-1}$ and a radius of curvature of 1000 mm. - The wheelchair, with user and possibly maximum extra weight of 10 kg and sticking out less than 20 cm (e.g. medical equipment or groceries) must not tip over on uneven terrain with a maximum slope of 30 degrees. - The device must only require maintenance, regular checks, repairs and replacements of worn out or damaged parts once a year. - The wheelchair must not require more than 20 N to be propelled by the user itself. - The wheelchair must be easily collapsible to 75% of its original volumetric dimensions by nine out of 10 nurses within 2 minutes, provided a manual and training. - The wheelchair must be adjustable. - The wheelchair frame must not weigh more than 16 kg.
Should have	- The wheelchair should not be more visible than 25% of the total frontal view and 60% of the total side view (i.e. see person and not wheelchair) as well as at least 75% of the user must be visible from the side view. - The wheelchair should be as cheap as possible.

	Description
	- The wheelchair should provide multiple power assistance magnitudes, i.e. 0%, 25%, 50%, 75% and 100% of maximum output motor. - The wheelchair should not have any sharp edges or protrusions. - The wheelchair should be ergonomic. - The wheelchair should be as lightweight as possible. - The wheelchair should be collapsible to 50% of the original volumetric dimensions by nine out of 10 nurses within 2 minutes, provided a manual and training.
Could have	- The wheelchair could have armrests - The wheelchair could have reflective units.
Won't have	- The wheelchair won't have a seatbelt - The wheelchair won't have a usb port to charge a phone.

3. Synthesis Phase I

3.1 Morphological map

A morphological map provides an overview of product functionality and characteristics and provides alternative combinations of achieving functionality. The morphological map is the basis for pre concept design and can be seen in table 6 for a PAPAW.

Table 6: Morphological map PAPAW

	1	2	3	4	5	6
Motor	DC current	Stepper	Hydraulic	Pneumatic		
Battery (energy source)	NiCd	NiMh	LiCoO2	LiMiMnCoO2	Manual	Pressurized gas from air compressor
Torque transmission	Conical gears	Cylindrical gears	Worm gears	Spur gears		
Anti tip mechanism	Anti tip wheels	Counter weight	Weight distribution	Camber	Gyroscopic stabilization technology	
Brake system	Manual on the pushrim	Brake on tire				
Adjustability	push button locking	Bolt and nut				
Portability	Lightweight	Foldable	Compact design			
Wheels	Solid pneumatic	Air-filled pneumatic				

3.2 Pre concepts

The focus of this thesis is on optimizing the design of current available PAPAW's such that tipping occurs less frequently. Therefore a completely novel device will not be introduced in this thesis. A normal foldable wheelchair base, inspired by the quickie 2 foldable manual wheelchair design, is used in all pre concepts and is presented below [14]. All concepts are equipped with the same equally powered DC motors and spur gear torque transmission, meaning all wheelchairs require roughly the same amount of force to be applied for movement. The batteries included are the same for all concepts and are AA 1.5 volt batteries. The actual wheelchair uses lithium cobalt oxide ($LiCoO_2$) batteries, because they offer high power and are relatively lightweight. In order to highlight the anti tipping intervention of the pre concept these features are not always drawn, however all pre concepts still have these features.

Base structure

The basic structure used for the pre concepts is made of PVC and PLA and consists of a collapsible frame that is adjustable in all dimensions and is depicted in figure 7. This allows for on the fly adjustments to be made to optimize structural stability.

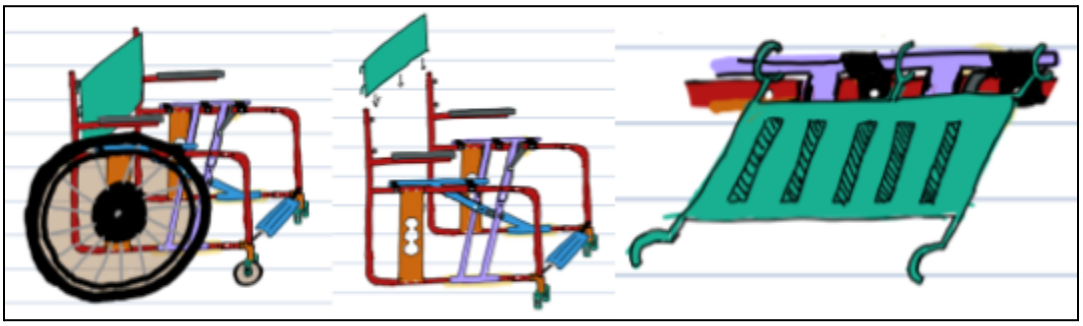

Figure 7: Base structure with wheels (left), without wheels (middle) and seating (right).

The wheel height and placement can be changed due to three different holes in the wheel holder for the wheel axis as can be seen in figure 8.

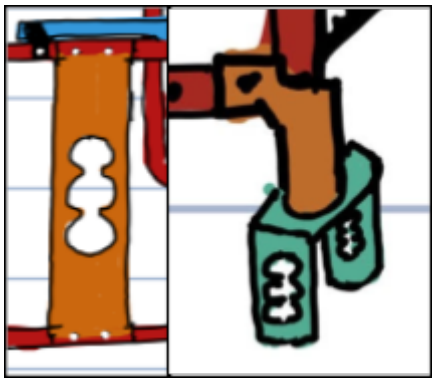

Figure 8: Variable placement options for big wheel (left) and small wheel (right).

The base wheelchair structure is extendable in terms of width and length using bolts and nuts. The length of the wheelchair is adjusted by extending the red pipes at the front of the chair (figure 9; left). The width of the wheelchair is adjusted by removing the pin connecting the purple and blue pipes and extending the pipes consequently (figure 9; right). After the pipes are extended to the desired length the pin is once again inserted.

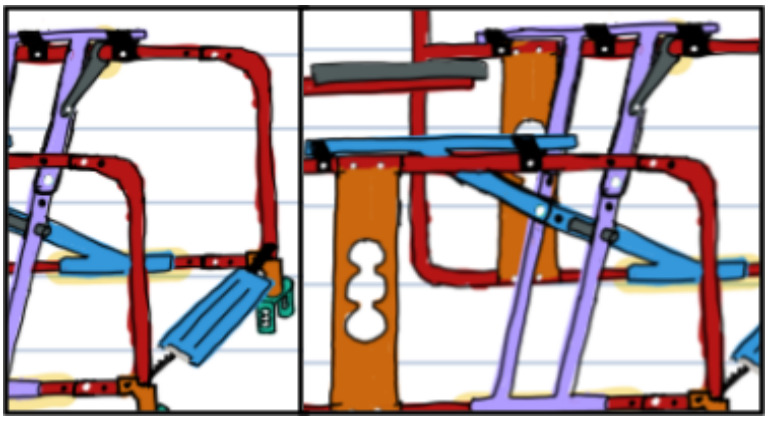

Figure 9: Extendability wheelchair length (left) and extendability wheelchair width (right).

All pre concepts are possible improvements added to the base structure and introduce a way to reduce tipping probability.

3.2.1 Pre-concept 1

The first pre concept involves collapsible anti tip wheels to the rear and lateral sides of the wheelchair. The aim of these wheels is to create a new wider POC, when needed, to prevent rear and lateral tipping. These cantilever structured anti tipping devices allow for a greater tipping angle and can be attached to the wheel axis or the lateral structure of the wheelchair. However, these added wheels have to be able to endure a lot of force once they are used and make the wheelchair wider. Typically these anti tipping wheels are not very shock absorbent and therefore air-filled wheels can also be considered for this prototype (figure 10; right).

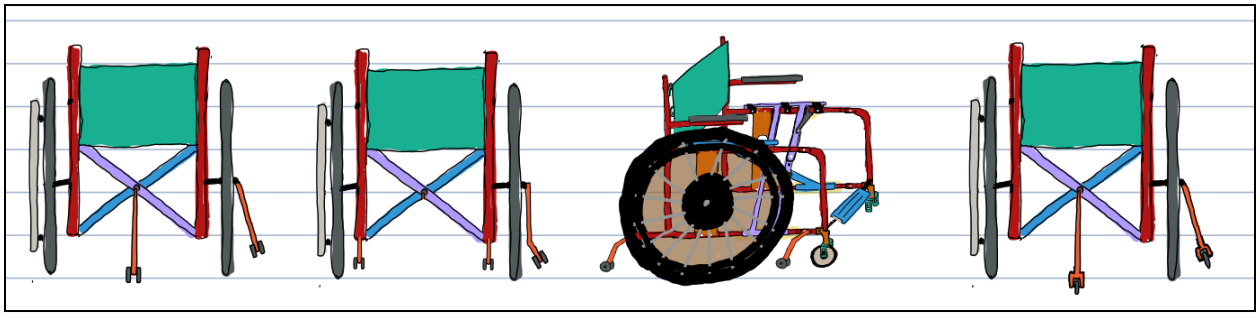

Figure 10: Different ways of attachment of anti tipping wheels.

3.2.2 Pre-concept 2

The second pre concept involves optimizing weight distribution by motor and battery placement. The goal is to lower the center of gravity as much as possible, therefore the batteries and motors must be placed as low as possible. The three most viable options for motor placement are: attached between the inner part of the wheel holders (figure 11; left), attached to the wheels (figure 11; middle), attached to the inner part of the wheel holders (figure 11; right). The two most viable options for motor placement are: inside the front red tubes of the structure (structure acts as housing) and inside the lower part of the structure. This can be seen in figure 11, where a motor is depicted as gray with a pink 'M' and a battery is depicted as gray with a pink 'B'. It should be noted that certain placement of motors and batteries can influence adjustability and collapsibility.

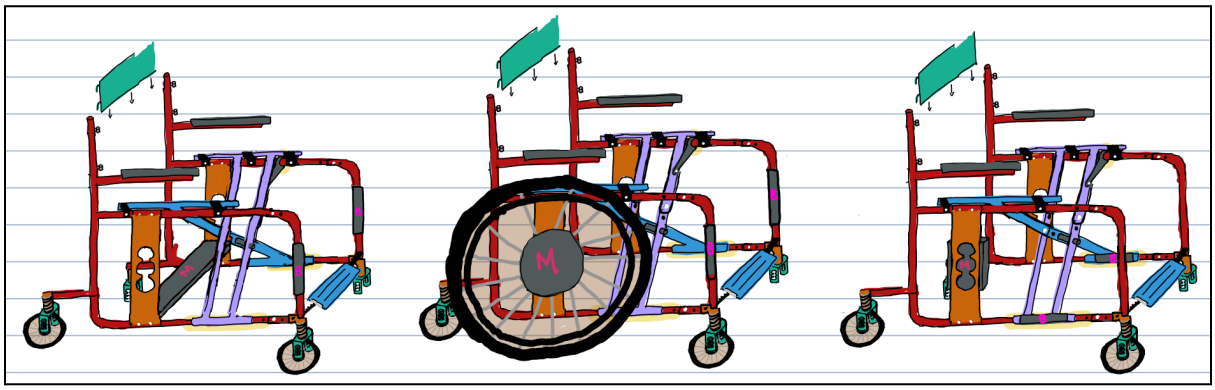

Figure 11: Different options of attachment of battery and motor placement.

3.2.3 Pre-concept 3

The third preconcept is about lowering the center of gravity by making the lower base of the wheelchair heavy. This can be done through the use of metals like aluminum and steel. Also extra weight can be added in the pipes. Even though this adds undesired extra weight to the wheelchair it does reduce the tipping probability and makes the wheelchair more stable. The pipes that would be weighted can be seen in figure 12.

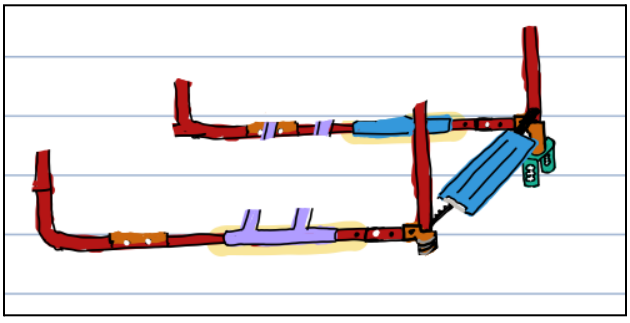

Figure 12: Adding extra weight to the lower base of the wheelchair.

3.2.4 Pre-concept 4

The fourth preconcept uses negative camber in the wheels to widen the base of the wheelchair and thereby reduce tipping probability and increase wheelchair stability and is depicted in figure 13. This technique is typically used in sports wheelchairs, but it is not common in manual wheelchairs [18]. This has to do with ergonomics. Changing the camber on the wheels changes the pushing motion of the user and thereby changes the strain put on the shoulder, elbow and wrist joints. The most optimal camber in terms of ergonomics for normal usage of a manual wheelchair is typically between 0 and 3 degrees [19]. It has been shown that negative camber has a very small effect on rolling resistance as the recorded rolling resistances were 8.74 N, 8.3 N, 8,22 N and 7.55 N for 0, 3, 6 and 9 degrees camber respectively. It was also shown that camber between 0 and 9 degrees has no significant kinematical or physiological effects, such as changes in mechanical efficiency, heart rate and metabolic cost [20].

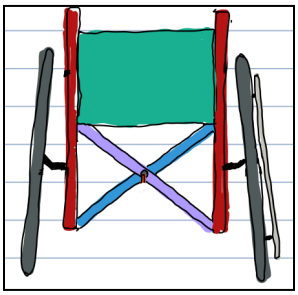

Figure 13: Negative camber in wheels.

3.2.5 Pre-concept 5

The fifth and final preconcept utilizes a gyroscopic stabilization technology (GST) to prevent tipping. It uses a gyroscope and accelerometers to continuously monitor the tilt and movement of the wheelchair. An algorithm processes the data from the sensors and calculates the necessary corrective actions for stabilization. Subsequently, an actuator with counterweights provides the force for stabilization based on the feedback given by the algorithm, which is acquired by sensor data. This GST system is mounted to the wheelchair frame under the seat or bottom of the frame as can be seen in figure 14.

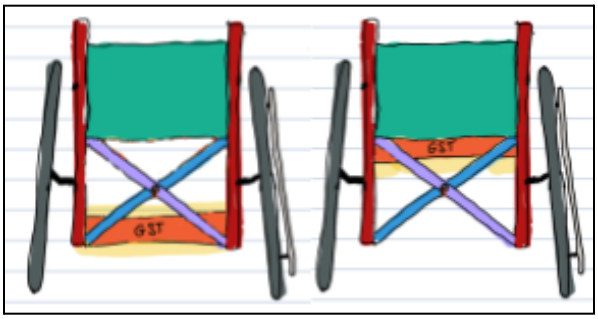

Figure 14: GST system mounted to bottom of frame (left) and underneath seat (right).

3.3 Pre-concept selection

The pre concepts were graded for all requirements and wishes using a grading scale from 1 to 5. A score of 1 refers to the requirement or wish not being fulfilled and a 5 means it is very well fulfilled. Each grade was multiplied by the weighting dictated by relative importance of the requirements and wishes, providing a weighted total score. If a grade could not yet be assigned the category was marked with an 'x'. The grades for all wishes and requirements are presented in table 7-13.

3.3.1 Function requirements (R) and wishes (W)

Table 7: Pre concept scores based on function

	R1 (x10)	R2 (x6)	R3 (x7)	R4 (x9)	W1 (x4)	W2 (x2)	W3 (x1)	Total
Pre concept 1	5	4	4	4	5	3	1	**167**
Pre concept 2	5	5	5	4	5	4	1	**178**
Pre concept 3	5	5	5	4	5	4	1	**178**
Pre concept 4	5	4	4	5	5	3	1	**172**
Pre concept 5	5	2	2	4	5	1	1	**135**

Foldability and adjustability is expected to be more complex and limited with the introduction of cambered wheels (preconcept 4) as well as the addition of side wheels (pre concept 1) and GST due to the attachment location (preconcept 5) (R3).

3.3.2 Safety requirements (R) and wishes (W)

Table 8: Pre concept scores based on safety

	R1 (x10)	R2 (x10)	W1 (x4)	W2 (x1)	Total
Pre concept 1	5	x	5	5	**75**
Pre concept 2	5	x	5	5	**75**
Pre concept 3	5	x	5	5	**75**
Pre concept 4	5	x	5	5	**75**
Pre concept 5	5	x	5	5	**75**

It is expected all prototypes are equally safe because of the same base frame without any sharp edges (R1). Tipping probability is yet to be determined during tests (R2) and can therefore not yet be assessed.

3.3.3 Performance requirements (R) and wishes (W)

Table 9: Pre concept scores based on performance

	R1 (x8)	R2 (x8)	R3 (x9)	Total
Pre concept 1	x	x	5	**45**
Pre concept 2	x	x	5	**45**
Pre concept 3	x	x	5	**45**
Pre concept 4	x	x	5	**45**
Pre concept 5	x	x	5	**45**

Tipping probability is to be determined in tests (R1 and R2) and can therefore not yet be graded. All wheelchairs are expected to have similar drag and friction, with a negligible difference, meaning the battery runtime will be the same for all pre concepts.

3.3.4 Usage requirements (R) and wishes (W)

Table 10: Pre concept scores based on usage

	R1 (x8)	W1 (x4)	W2 (x2)	Total
Pre concept 1	5	x	5	**50**
Pre concept 2	5	x	5	**50**
Pre concept 3	5	x	5	**50**
Pre concept 4	5	x	5	**50**
Pre concept 5	5	x	5	**50**

Ergonomics are based on seating and back cushions as well as posture and are distinctive for each user and can therefore not be assessed.

3.3.5 Time requirements (R) and wishes (W)

Table 11: Pre concept scores based on time

	R1 (x9)	R2 (x8)	Total
Pre concept 1	x	4	**32**
Pre concept 2	x	5	**40**
Pre concept 3	x	5	**40**
Pre concept 4	x	4	**32**
Pre concept 5	x	4	**32**

R1 can not be rated as it requires observing the performance of the wheelchair over a period of 7 years. It is expected that camber and GST require more maintenance due to the nature of the technological complexity (R2)[21]. Also side wheels are expected to be more prone to destructive events due to the high forces acting on the wheels when used (R2).

3.3.6 Size requirements (R) and wishes (W)

Table 12: Pre concept scores based on size

	R1 (x10)	R2 (x6)	W1 (x5)	W2 (x3)	Total
Pre concept 1	4	5	3	5	**80**
Pre concept 2	5	5	5	5	**100**
Pre concept 3	5	4	5	4	**91**
Pre concept 4	4	5	4	5	**85**
Pre concept 5	5	3	4	3	**82**

The use of counterweights in GST as well as making a heavy base as in concept 3 is expected to significantly add to the weight. Given the time constraint of the project of 10 weeks, all prototypes will have the 2 identical motors. Use of 1 or more than 2 motors will not be tested.

3.3.7 Cost requirements (R) and wishes (W)

Table 13: Pre concept scores based on cost

	W1 (x5)	Total
Pre concept 1	5	**25**
Pre concept 2	5	**25**
Pre concept 3	5	**25**
Pre concept 4	4	**20**
Pre concept 5	2	**10**

Cambered wheels and GST are relatively expensive compared to the other prototypes [21].

3.3.8 Weighted total scores

Based on all the requirements and wishes that could be graded the weighted total scores were noted in table 14.

Table 14: Pre concept scores weighted totals

	Pre concept 1	Pre concept 2	Pre concept 3	Pre concept 4	Pre concept 5
Total score	474	**513**	504	479	429

It can be seen that preconcept 2 has the highest score and is therefore most probable to be most successful. However, dynamic tipping tests are not yet taken into account, which could affect the preconcept score.

4. Synthesis Phase II

4.1 Detailing

Scaling

All quantities involved in a wheelchair design, such as mass, volumetric dimensions and motor power are scaled down to a 3.5 : 1 ratio compared to the actual size. The primary reason for the scale factor has to do with spatial limitations. The testsite consists of one table of approximately 2.5 m by 1 m. Thus, in order to test whether the wheelchair can make a rotation with a radius of curvature of 1000 mm with a velocity of 6 $km\ h^{-1}$ the right ratio has to be calculated. This means the maximum size dimensions as a result of the scaling factor for the prototype become 228 mm, 285.7 mm and 257.1 mm (WxLxH) . Also the speed at which a radius of curvature of 81.63 mm has to be taken without tipping becomes 0.48 $m\ s^{-1}$. This scaled radius of curvature ($r_{test,\ scale}$) can be calculated by rearranging formula 9 into a formula 10 and inserting 1000 mm for $r_{test,\ real}$ [12]. This calculation considers the quadratic nature of the centrifugal forces acting on the actual wheelchair as a function of velocity in order to simulate the same centrifugal forces in the model and can be seen below.

$$r_{test,\ scale} = \frac{(\frac{v_{real}}{3.5})^2 * 2\frac{h}{3.5}}{\frac{b}{3.5}g} = \frac{v_{real}^2 * 2h}{3.5^2 * bg} = \frac{r_{test,\ real}}{3.5^2}; \qquad (10)$$

In this thesis a wheelchair structure mass of a maximum of 16 kg and electronics weight of approximately 5 kg is considered, which scales down to a total model mass of approximately 6 kg. Thus in order to reach a speed of 0.48 $m\ s^{-1}$, considering the scaled mass and test space dimensions, the motors must be able to provide a combined power output of approximately 3.2 W, which translates to a torque of 0.085 Nm in order to overcome friction and mass inertia of the wheelchair. The calculation is given below.

Power, torque and acceleration estimation and calculation

The diameter of the large wheels is 0.17 m, meaning the circumference of this wheel is 0.53 m. This means the revolutions per minute (RPM) of the wheel must be equal to 54.35 rpm to obtain a linear velocity 0.48 $m\ s^{-1}$ (v). This can be calculated by filling in formula 11 [10].

$$RPM = \frac{v}{circumference} * 60\ ; \qquad (11)$$

This means the angular velocity of the wheels will be equal to 5. 69 $rad\ s^{-1}$using formula 12 [10]. Where r_{wheel} is the scaled radius of the wheel.

$$\omega = \frac{v}{r_{wheel}} = \frac{2\Pi * RPM}{60}\ ; \qquad (12)$$

The wheel is geared on a 17:1 ratio relative to the RPM of the motor shaft, which can be done using spur gear torque transmission (1 gear on motor shaft and 1 wheel of a diameter of 17 cm). This ratio has a maximum RPM of 541 rpm, which is sufficient, since it is more than the required RPM of 54. 35 rpm. The maximum torque output of the motor shaft (τ_{Motor}) is 5 mNm, meaning the torque output at the wheel (τ_{Wheel}) at this gear ratio is equal to 0.085 Nm at full motor power. The motors being used produce a maximum power of 3.2 W with 6 V, with the amount of torque being related to the current and the speed being determined by the applied voltage output

The total force (F_{tot}) generated tangent to the wheel as a result of the torque is equal to 1 N and can be calculated using formula 13, where $\tau_{Wheel} = 0.085\ Nm$ and $r_{wheel} = 0.085\ m$ [10].

$$F_{tot} = \frac{\tau_{Wheel}}{r_{wheel}}\ ; \qquad (13)$$

The total force is composed of a rolling resistance force (F_r) and a resulting acceleration force (F_a), which can be seen in formula 14. However, this does not consider additional friction, which will be determined experimentally [22].

$$F_{tot} = F_a + F_r\ ; \qquad (14)$$

The rolling friction coefficient (μ_r) pneumatic wheelchair wheels on concrete is roughly 0.01, which scales down to 0.003 due to less contact area [23]. The normal force (F_N) is roughly equal to 58 N, since the electronics are estimated to have a scaled mass of roughly 1.5 kg. From this the scaled rolling resistance is estimated to be ~0.177 N and can be calculated using formula 15, where μ_r = 0.003 and F_N = 58 N [22].

$$F_r = \mu_r * F_N; \qquad (15)$$

Since the amount of torque required to overcome the mass inertia is equal to the resistance ($\tau_{Required} = \tau_{Rolling} = 0.015\ Nm$), it can be seen that the motors have enough torque to overcome the rolling resistance (τ_{wheel} (0.085 Nm) > $\tau_{Required}$ (0.015 Nm)). The required torque is found by substitution of F_r in formula 12.

By substitution of F_{tot} and F_r into formula 14 one finds the resulting acceleration force to be 0.823 N. From this the acceleration (a) of the wheelchair can be calculated using formula 16, where F_a = 0.823 N and m = ~6 kg [22]. The acceleration of the wheelchair is equal to $0.137\ m\,s^{-2}$.

$$a = \frac{F_a}{m}; \qquad (16)$$

The time traveled to reach the desired linear velocity can be calculated from the acceleration and is given by formula 17. By filling in the equation with $v = 0.48\ m\,s^{-1}$ and $a = 0.137\ m\,s^{-2}$ one finds the time to be equal to $3.5\ s$ [10].

$$t = \frac{v}{a}; \qquad (17)$$

During the 3.5 seconds that the torque is applied to the wheels, the distance traveled without friction will approximately be 0.84 m. This can be found using formula 18, which describes velocity as a function of power as a function of time [22].

$$v(t) = \frac{P(t)}{F_{tot}} = \frac{(m*a)(a*t)}{F_{tot}} = \frac{ma^2t}{ma} = at = 0.137t\ ms^{-1}; \qquad (18)$$

As distance is a time derivative of distance, the traveled distance during the 3.5 seconds to reach power of $3.2\ W$ and a velocity of 0.48 $m\,s^{-1}$ can be found using the integral. The distance traveled is 0.84 m and was obtained by inserting τ = 3.5 into formula 19 and solving this equation [10].

$$s(t) = \int_0^{\tau} v(t)dt = \int_0^{\tau} 0.137tdt; \qquad (19)$$

Dynamic tests are performed on a table that is 2.5 m in length, which is enough space, since the wheelchair uses 0.84 m to obtain the desired testing speed. However, it should be noted that there is also friction acting on the axis of the wheel as the structure leans on it. This friction is not considered in the calculation and results in less efficiency. This means the acceleration will be lower in the tests and is determined experimentally.

Experimental acceleration and friction

In practice, it took the base 3.4 s to cover a distance of 0.654 m. This results in an average velocity of $0.19\ ms^{-1}$, which is calculated using formula 19 [12]. The tests were performed at this speed due to spatial limitations.

$$v_{avg} = \frac{v_{final} - v_{start}}{2}; \qquad (19)$$

This means the wheelchair has an actual acceleration of $0.057\ ms^{-2}$ and a final velocity of $0.38\ ms^{-1}$, which can be calculated using formula 16 and 19 respectively. Using this acceleration in formula 15 results in the actual acceleration force to be 0.342 N. This means the frictional force (F_f) acting on the wheelchair is 0.481 N, which is a 59% decrease in motor power efficiency [24]. This frictional force primarily comes from the weight acting on the wheel axis, because this design does not use a bearing. Also power is lost in the gears due to friction.

An overview of all relevant scaled dimensions and quantities can be seen in table 15.

Table 15: Scaled dimensions and quantities of wheelchair prototype.

	Scaled dimensions
Length	285.7 mm
Height	257.1 mm
Width	228 mm
Weight	~6 kg
Testing speed	$0.38\ m\ s^{-1}$
Effective power motors	~3.2 W
Motor voltage	6 V
Torque at wheel (τ_{wheel})	0.085 Nm
Accelerating force (F_a)	0.342 N
Rolling resistance (F_r)	0.177 N
Friction (F_f)	0.481 N

Testing setup

To evaluate wheelchair stability, both static and dynamic stability tests were conducted on the prototypes. All tests were conducted once and a measurement error was added (standard deviation).

Static tests

The static tipping angle was first tested by placing the wheelchair on a level surface and gradually increasing the surface angle with 1 degree increments until the wheelchair began to tip, as depicted in figure 15. This procedure was performed in front, rear and lateral direction ($\Theta_{tip,\,front}$, $\Theta_{tip,\,rear}$, $\Theta_{tip,\,lateral}$). The wheelchair is put on brake using tie wraps to prevent it from rolling during the tests. Also a small curb is placed to secure the wheelchair and prevent the wheelchair from sliding down.

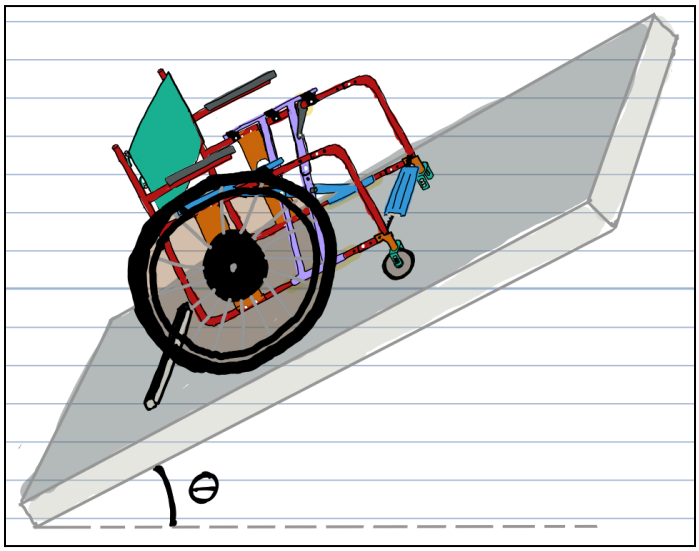

Figure 15: test setup for static tilt angle (θ).

Dynamic tests

The dynamic tests involved assessing the wheelchair stability at a speed of 0.48 $m\,s^{-1}$ while navigating a radius of curvature of 81.63 mm. The wheelchair is expected to maintain stability at this speed without tipping. However, it was tested at a speed of 0.38 $m\,s^{-1}$, which was the maximum speed the wheelchair is able to reach within the limited space.

Additionally, the wheelchair was tested for maximum acceleration at which stability was maintained on different surface angles ($\Theta_{tip,\,acceleration}$) in 1 degree increments, as shown in figure 16. This was done by setting the power to 100% from standstill.

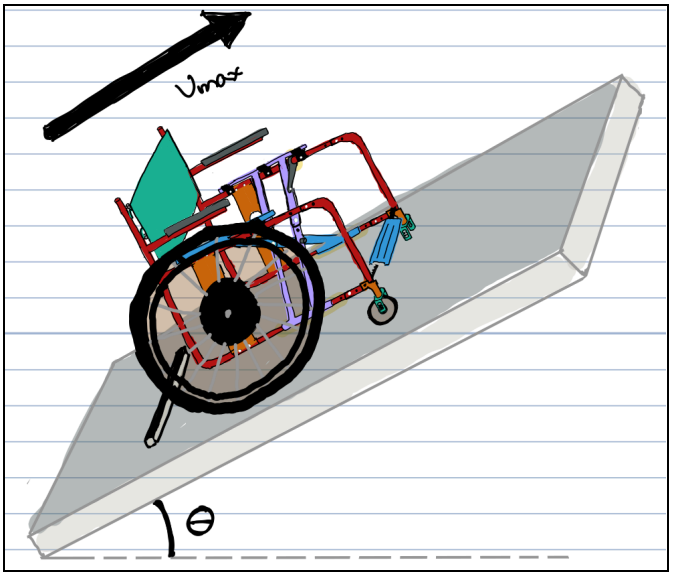

Figure 16: test setup for maximum acceleration.

Lastly the wheelchair was tested on small curbs that simulated a transition from pavement to the street. Stability was observed at 3 different approach angles (90 degrees, 60 degrees and 30 degrees) and two different curb heights of 50 mm and 70 mm, which are scaled heights slightly larger than average Dutch pavements [25]. The tests were quantified using a binary system, 1 being the wheelchair maintained stability and 0 being the wheelchair has tipped over. Also, if applicable it is mentioned which way the wheelchair has tipped. Front tipping was denoted with 'F', lateral tipping with 'L' and backwards tipping with 'B'. This test was performed at a speed of 0.38 $m\ s^{-1}$ going down the curb and can be seen in figure 17.

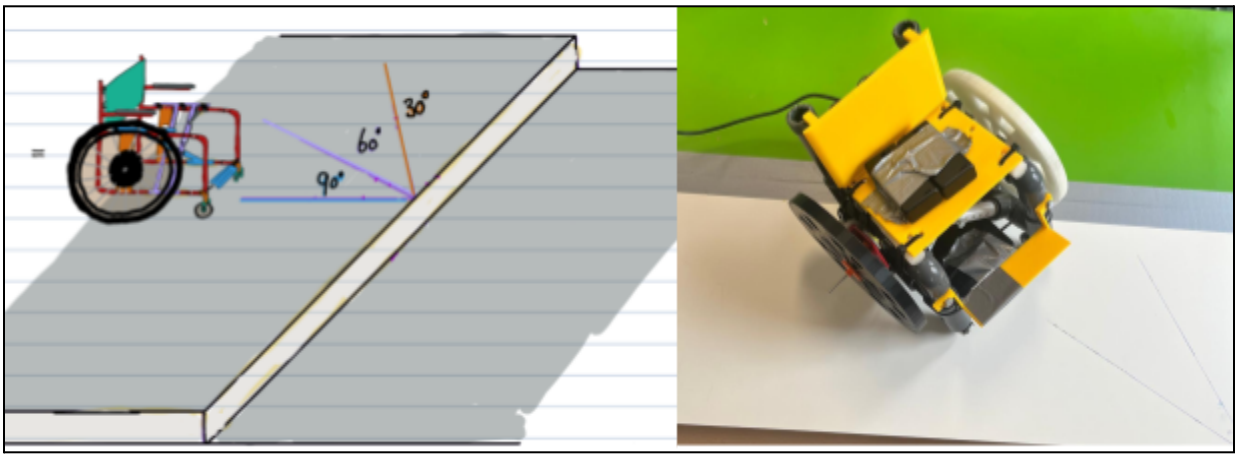

Figure 17: test setup for curb testing.

4.2 Sprints

The prototypes were tested in several sprints. A sprint refers to the process of building a prototype and testing it.

4.2.1 Design sprint 1 (base structure)

Sprint 1 used the base structure and investigated the wheelchair width, length and height as a function of tipping probability, with the objective of determining the significance of a change in one of these dimensions.

The base wheelchair was constructed using PVC and PLA and was assembled using both press fits as well as bolts and nuts. Additionally, the PVC pipes were glued into the connecting PVC pieces (T-pieces and bends) for supplementary structural integrity. These materials were also used to make the rear wheels, because they are relatively cheap and strong. The smaller front wheels were bought from the Gamma (product number: 840025). The seat, backrest and footrest were all printed using a 3D printer. The electronics consisted of 2 equally powered DC motors, an arduino uno board, batteries and an H-bridge. The H-bridge controls the direction of the motor by inverting the current using switches. The motor was connected to the structure using tie wraps for the prototype. A real sized model would require galvanized PVC brackets or wheel holders in order to fixate the motor and wheel. The CAD design of the base wheelchair can be seen in figure 18a and the actual model can be seen in figure 18b.

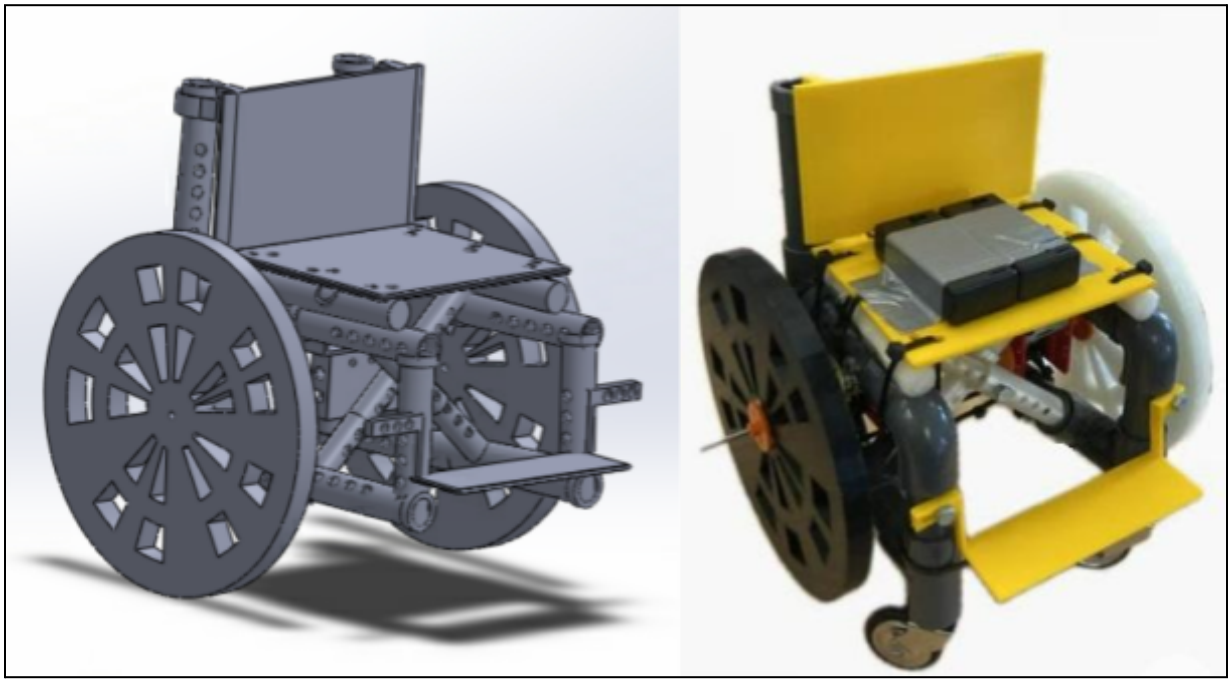

Figure 18: Base structure wheelchair.

The wheels were not pneumatic nor covered with rubber on the outside to avoid excessive friction, which the power supply could not overcome. The metric dimensions of the wheelchair in terms of length (L), width (W) and height (H) of the base structure that were adjusted are presented in figure 21.

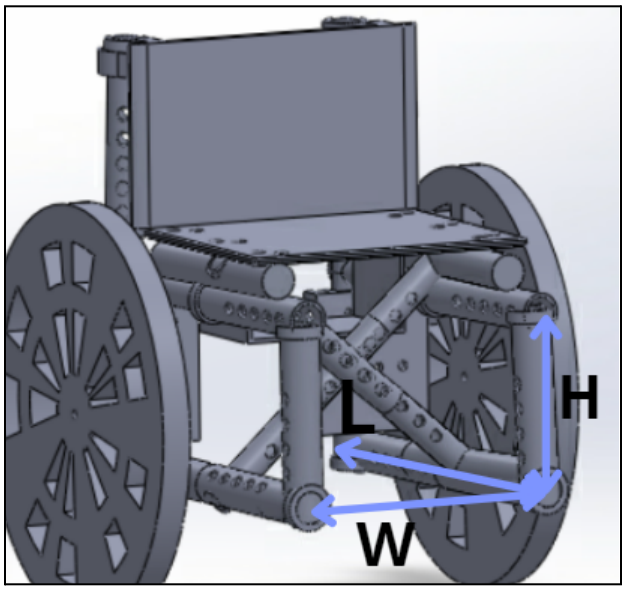

Figure 21: changeable dimensions.

Electronics (motors)

The wheelchair employed two identical motors that had a combined power capacity of 3.2 W at 6 V. The motors are 1.62 W brushless DC motors from RS (RS number: 238-9844). The torque was transmitted using 1 : 17 spur gear transmission, as illustrated in figure 19, resulting in an output torque of the motor of 5 mNm and output speed of 2300 RPM.

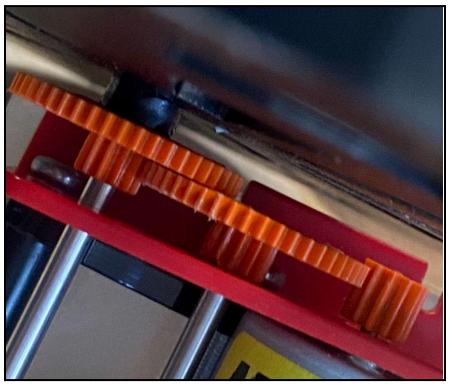

Figure 19: Spur gear transmission.

The average amount of voltage supplied was regulated using pulse width modulation (PWM), meaning the battery supplied the H-bridge with 6 V, which in turn supplies each motor with the effective voltage based on the pulse magnitude and frequency. The circuit diagram, consisting of

the H-bridge, motors, power supply and arduino pin connections can be seen in figure 20.

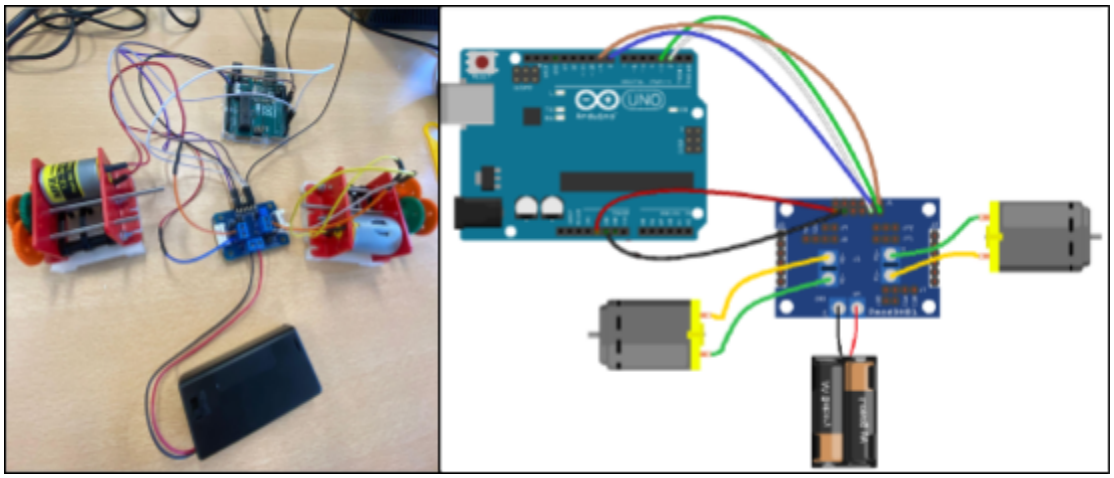

Figure 20: Actual H-bridge and arduino connections (left) and schematic circuit diagram (right).

The motor was run using the command 'bm forward xx yy' or 'bm backward xx yy' in the arduino serial monitor followed by the percentage of motor power required, where 'xx' and 'yy' refers to the motor power of motor 1 and motor 2 respectively. The arduino code to power the motors is provided in the appendix B. This code was taken from a project by Martha Miglacio and Alex Wong (2017) [26]. However, this code was modified in order to be able to drive both motors with one command using 'bm forward xx yy' or 'bm backward xx yy'.

These electronics were then placed in a compartment underneath the seating using double sided tape as can be seen in figure 21.

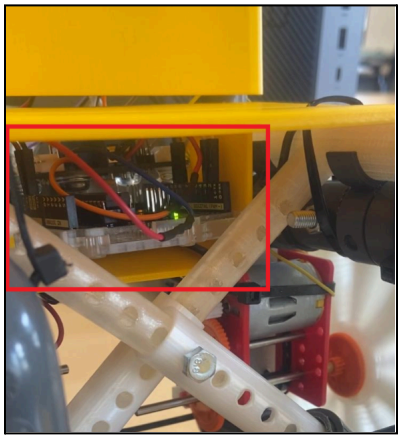

Figure 21: electronics placement.

The USB cable connecting the arduino to the laptop was inserted into the arduino on the rear side, such that it did not hinder the movement during the stability tests.

4.2.2 Testing sprint 1

Static tests

The dimensions were tested in several length, width and depth configurations to determine the optimal wheelchair dimensions. The following dimension configurations (LxWxH) were tested.

Table 16: Different volumetric dimensions being tested in different configurations for sprint 1.

	Length [mm] ± SD	**Width [mm] ± SD**	**Height [mm] ± SD**
Configuration 1	220 ± 5	200 ± 5	230 ± 5
Configuration 2	220 ± 5	220 ± 5	230 ± 5
Configuration 3	230 ± 5	200 ± 5	230 ± 5
Configuration 4	220 ± 5	200 ± 5	248 ± 5

*SD = standard deviation

Tipping angles of these configurations can be seen in table 17. The seat is tilted back ~5 degrees in the first 3 configurations due to the wheel being 17 cm in diameter. For a wheel with a diameter of 19 cm the seat angle is completely level (configuration 4).

Table 17: Static tipping angle in degrees of base structure for variable width, length and depth for sprint 1.

	Config 1	**Config 2**	**Config 3**	**Config 4**
$\Theta_{tip,\,front}$ ± SD	41 ± 1	40 ± 1	42 ± 1	35 ± 1
$\Theta_{tip,\,rear}$ ± SD	10 ± 1	10 ± 1	12 ± 1	12 ± 1
$\Theta_{tip,\,lateral}$ ± SD	40 ± 1	42 ± 1	40 ± 1	43 ± 1

*SD = standard deviation

Dynamic tests

The base structure was also tested for velocity for a radius of curvature of 81.63 mm without tipping. These results are presented in table 18. Configuration 4 was only tested statically by placing the rear wheels on a wooden plank to increase height. Dynamical tests to investigate the effect of height on tipping probability would require a larger wheel to be made.

Table 18: maximum velocity in meters per second for radius of curvature of 81.63 mm for sprint 1.

	Config 1	Config 2	Config 3	Config 4
$v_{curv}\,(ms^{-1}) \pm$ SD	0.38 ± 0.3	0.38 ± 0.3	0.38 ± 0.3	X

*SD = standard deviation

The maximum surface angles could not be tested at maximum acceleration, due to insufficient torque in the wheelchair.

Lastly the wheelchair was tested going down a curb with the height of 50 mm and 75 mm. These results can be seen in tables 19 and 20.

Table 19: tipping test on a curb of 50 mm at 30, 60 and 90 degree angles for sprint 1.

	Config 1	Config 2	Config 3	Config 4
30°	1	1	1	X
60°	0 (B)	0 (B)	0 (B)	X
90°	0 (F)	0 (F)	1	X

** (B) = backward tip, (F) = front tip and (L) = lateral tip.*

Table 20: tipping test on a curb of 70 mm at 30, 60 and 90 degree angles for sprint 1.

	Config 1	Config 2	Config 3	Config 4
30°	1	1	1	X
60°	0 (B)	0 (B)	0 (B)	X
90°	0 (F)	0 (F)	0 (F)	X

** (B) = backward tip, (F) = front tip and (L) = lateral tip.*

4.2.3 Design sprint 2

For the second sprint the same base structure was used as in sprint 1 at 200 mm x 220 mm x 230 mm (WxLxH) to investigate battery placement in relation to tipping probability. The batteries were simulated using 4 x 15 g AA batteries and placed inside the frame at the bottom front end as can be seen in figure 22. Two batteries were placed on both sides and the exact placement can be seen indicated with red surfaces in figure 22c.

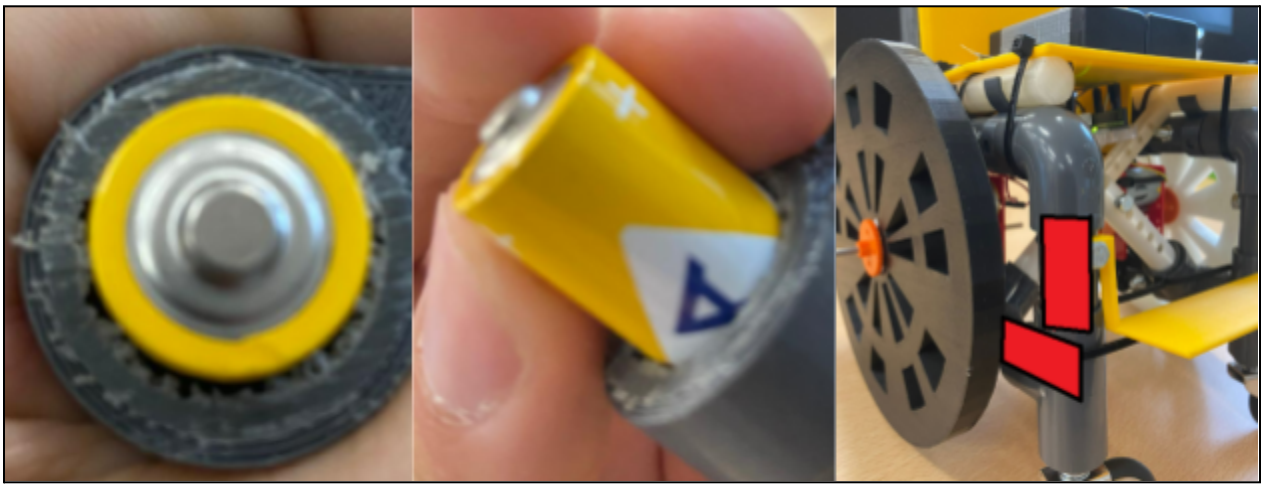

Figure 22: Battery placement.

4.2.4 Testing sprint 2

The static tip angles and maximum speed radius of curvature for sprint 2 were tested using the same methods as in sprint 1. The results can be seen in table 21.

Table 21: static tip angles and maximum speed radius of curvature for sprint 2.

	$\Theta_{tip,\,front} \pm$ SD	$\Theta_{tip,\,rear} \pm$ SD	$\Theta_{tip,\,lateral} \pm$ SD	$v_{curv} \pm$ SD
Sprint 2	38 ± 1	9 ± 1	40 ± 1	0.38 ± 0.3

*SD = standard deviation

The results from the tests with curbs of 50 and 70 mm heights similar to sprint 1 are displayed in table 22.

Table 22: tipping test on a curb of 50 mm and 70 mm height at 30, 60 and 90 degree angles for sprint 2.

	50 mm	**70 mm**
30°	1	1
60°	1	0 (F)
90°	0 (F)	0 (F)

** (B) = backward tip, (F) = front tip and (L) = lateral tip.*

4.2.5 Design sprint 3

For the third sprint the base structure was again used at 200 mm x 220 mm x 230 mm (WxLxH) to investigate the use of a heavy mass bottom base as a function of tipping probability. The bottom structure was weighted using a 194 g weight and placed on the bottom of the frame with equal weight distribution from the back to the front of the structure. This can be seen in figure 23.

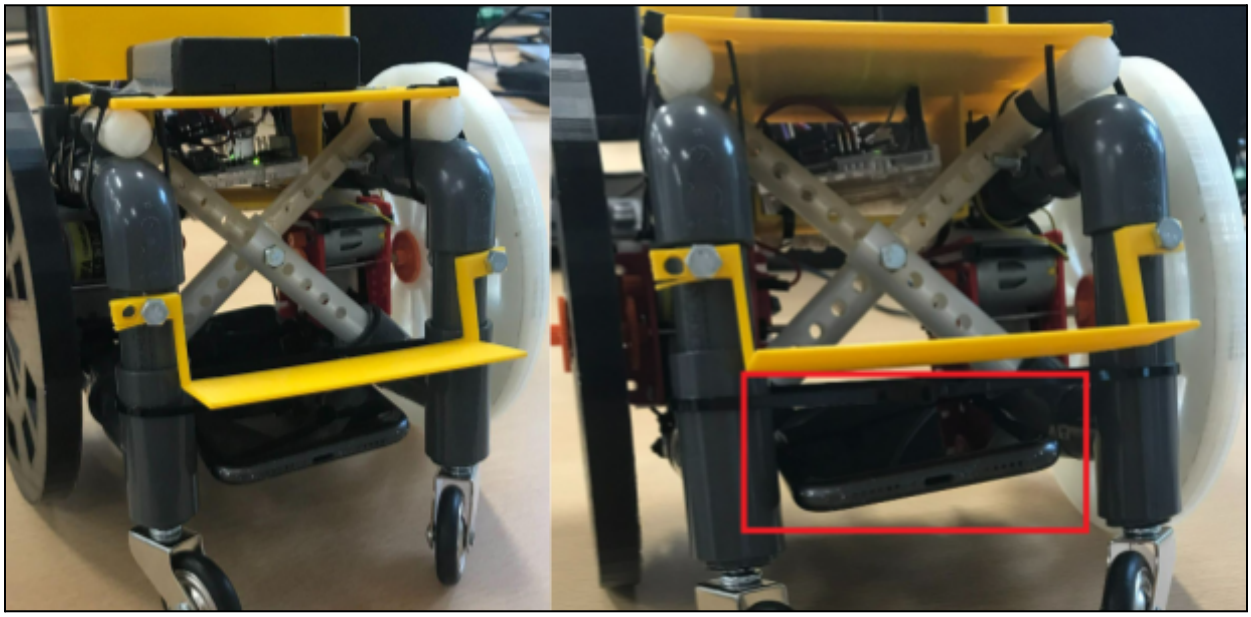

Figure 23: Heavy bottom structure.

The weight was held in place using tie wraps and duct tape.

4.2.6 Testing sprint 3

The static tip angles and maximum speed radius of curvature for sprint 3 were tested using the same methods as in sprint 1. The results can be seen in table 23.

Table 23: static tip angles and maximum speed radius of curvature for sprint 3.

	$\Theta_{tip,\,front} \pm$ SD	$\Theta_{tip,\,rear} \pm$ SD	$\Theta_{tip,\,lateral} \pm$ SD	$v_{curv} \pm$ SD
Sprint 3	45 ± 1	8 ± 1	44 ± 1	0.38 ± 0.3

*SD = standard deviation

The results from the tests with curbs of 50 and 70 mm heights similar to sprint 1 are displayed in table 24.

Table 24: tipping test on a curb of 50 mm and 70 mm height at 30, 60 and 90 degree angles for sprint 3.

	50 mm	**70 mm**
30°	1	0 (L)
60°	1	0 (B)
90°	0 (F)	0 (F)

** (B) = backward tip, (F) = front tip and (L) = lateral tip.*

4.2.7 Design sprint 4

For the fourth sprint the base structure was again used at 200 mm x 220 mm x 230 mm (WxLxH) to investigate the addition of anti tipping wheels as a function of tipping probability. The anti tipping wheels were only added to the rear side of the wheelchair (figure 24), since the lateral stability for the base structure has been proven to be sufficient. The anti tipping wheels were attached ~1 cm above the ground vertically and ~2 cm from the wheels horizontally.

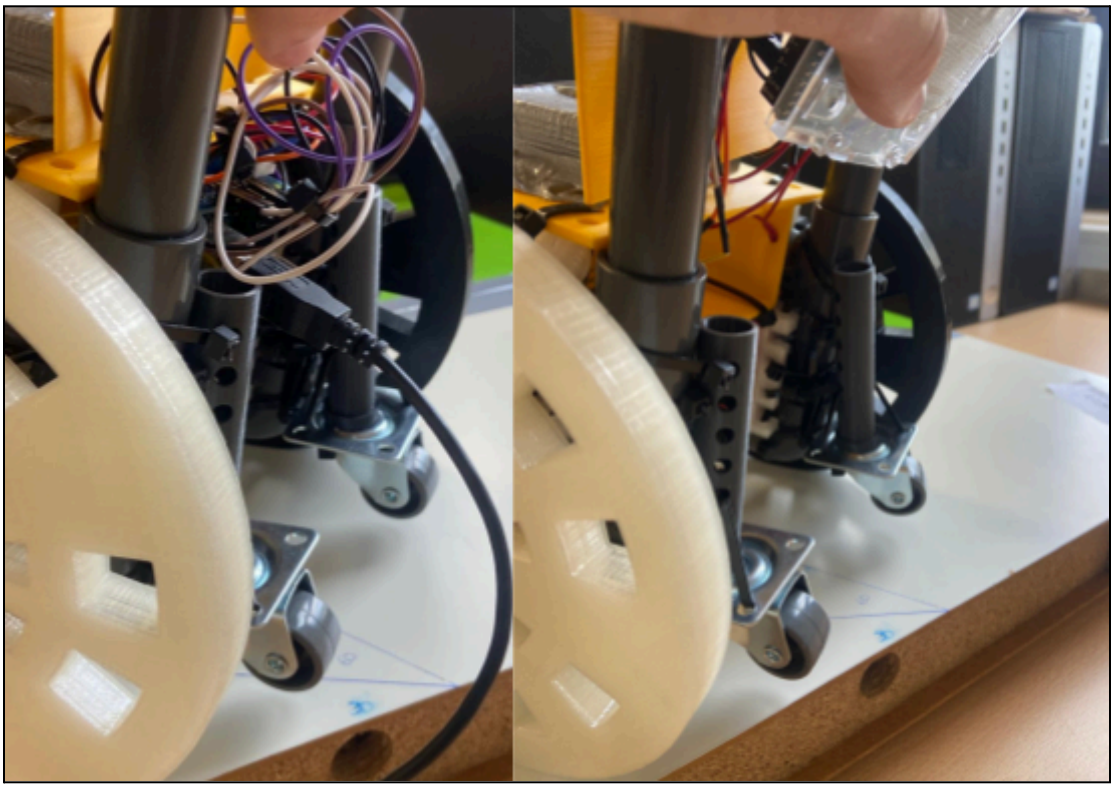

Figure 24: Anti tipping wheels.

The anti tipping wheels were bought from the gamma (product number: 100072) and connected to a 3D printed tube with tie wraps. This tube was in turn attached to the wheelchair structure using tie wraps.

4.2.8 Testing sprint 4

The static tip angles and maximum speed radius of curvature for sprint 4 were tested using the same methods as in sprint 1. The results can be seen in table 25.

Table 25: static tip angles and maximum speed radius of curvature for sprint 4.

	$\Theta_{tip,\,front} \pm$ SD	$\Theta_{tip,\,rear} \pm$ SD	$\Theta_{tip,\,lateral} \pm$ SD	$v_{curv} \pm$ SD
Sprint 4	47 ± 1	33 ± 1	42 ± 1	0.38 ± 0.3

*SD = standard deviation

The results from the tests with curbs of 50 and 70 mm heights similar to sprint 1 are displayed in tables 26.

Table 26: tipping test on a curb of 50 mm and 70 mm height at 30, 60 and 90 degree angles for sprint 4.

	50 mm	**70 mm**
30°	1	1
60°	1	1
90°	1	1

** (B) = backward tip, (F) = front tip and (L) = lateral tip.*

4.2.9 Overview results

Table 27 provides an overview of the critical angles measured for all sprints.

Table 27: Static tipping angle in degrees of all sprints.

	Sprint 1*	Sprint 2	Sprint 3	Sprint 4
$\Theta_{tip,\,front} \pm$ SD	39.5 ± 1	38 ± 1	45 ± 1	47 ± 1
$\Theta_{tip,\,rear} \pm$ SD	11 ± 1	9 ± 1	8 ± 1	33 ± 1
$\Theta_{tip,\,lateral} \pm$ SD	41.3 ± 1	40 ± 1	44 ± 1	42 ± 1

**For sprint 1 the average critical angles were calculated from the four configurations;* *SD = standard deviation

Figure 25 shows a Q-Q diagram of the results from table 27. This plot indicates the results do not follow a normal distribution and a one-way ANOVA can not be used, because the data points deviate from the 45 degree reference line [27].

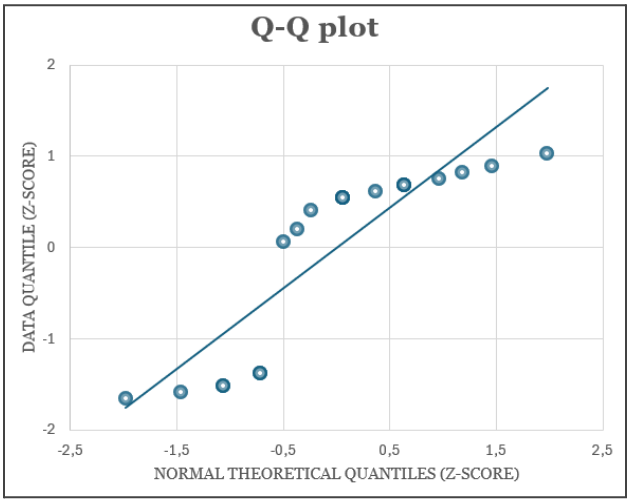

Figure 25: Q-Q plot of static tipping angles.

Therefore, a Kruskal-Wallis test was performed to test for significant differences in tipping angle between sprints [28]. The null hypothesis (H_0) and alternative hypothesis (H_a) were stated as follows using a significance level (α) of 0.05:

H_0: there is no significant difference in tipping angle.

H_a: there is a significant difference in tipping angle.

First the test statistic (H) was calculated using formula 20, where the sample size (n) = 12, the number of groups (k) = 4 and the rank sum for the ith group = R_i [29].

$$H = \frac{12}{n(n+1)} \sum_{i=1}^{k} \frac{R_i^2}{n_i} - 3(n+1) \qquad (20)$$

The H-statistic for the static tipping angles was 18.667 and the degrees of freedom (df) was 3. The p-value was calculated using the chi squared distribution function (1-stats.chi2.cdf(H , df)) in Python and equals 0.00032. This means the null hypothesis is rejected, which implies there is a significant difference in tipping angle between the sprints, (p < a (0.00032 < 0.05)). The code for this python calculation can be seen in appendix C [30].

An overview of the curb tests for all sprints with 50 mm and 70 mm curbs can be seen in table 28 and 29 respectively.

Table 28: tipping test on a curb of 50 mm at 30, 60 and 90 degree angles for all sprints.

	Sprint 1	**Sprint 2**	**Sprint 3**	**Sprint 4**
30°	1	1	1	1
60°	0 (B)	1	1	1
90°	0 (F)	0 (F)	0 (F)	1

** B = backward tip, F = front tip and L = lateral tip.*

Table 29: tipping test on a curb of 70 mm at 30, 60 and 90 degree angles for all sprints.

	Sprint 1	**Sprint 2**	**Sprint 3**	**Sprint 4**
30°	1	1	0 (L)	1
60°	0 (B)	0 (F)	0 (B)	1
90°	0 (F)	0 (F)	0 (F)	1

** B = backward tip, F = front tip and L = lateral tip.*

4.3 Discussion sprints

The addition of anti tipping wheels (sprint 4) and a lower center of mass (sprint 3) had a notably higher critical front tipping angle of at least 5 degrees more compared to the base structure, which was due to the adjusted weight distribution. In these sprints more weight was added to the rear side of the wheelchair, shifting the center of gravity to the rear and thereby reducing front side tipping probability. Lateral stability remained roughly consistent across all sprints. Lastly, it can be seen that adding anti tipping wheels increased the rear tipping angle by threefold. Thus addition of this feature results in a significant reduction of rear tipping probability.

Furthermore, from the dynamic curb tests it can also be concluded that anti tipping wheels are the most effective method to reduce tipping probability. For almost all curb tests, approaching the curb at a 30 degree angle the wheelchair did not tip, which is indicative of sufficient lateral stability. However, in the first two sprints tipping occurred at nearly all 60 and 90 degree approach angles for both curb sizes. The wheelchair in sprint 3 does perform well for the 50 mm curb (tipped 1 time out of 3 tests), nevertheless its performance becomes worse as the curb size increases to 70 mm (tipped 3 times out of 3 tests). It can be seen that the wheelchair in sprint 4 remained stable along all approach angles and curb sizes. Thus the prototype in sprint 4 had the lowest dynamical tipping probability in these curb tests, meaning it was most stable.

Based on the results of this thesis battery placement does not provide measurable differences in tipping probability nor do minor changes in dimensions. However, it is useful to lower the center of mass of a papaw as well as add anti tipping wheels to the rear of the wheelchair. These proposed interventions are cost-effective, comply with the requirements and wishes and reduce static and dynamic tipping probability in a PAPAW. These results comply with a study done by Kirby R.L. et al (1996), which investigates positions of anti tipping wheels as a function of maneuverability and tipping [31]. This study similarly proves the positive effect of anti tipping wheels on tipping probability and states that optimal placement of anti tipping wheels is different for each user. Furthermore, the results of sprint 3 comply with a study done by Thomas L. et al (2018), which investigated downhill wheelchair stability. This study found that lowering seat height and reclining the seat significantly reduces tipping probability [32]. These two interventions lower the CG, which was also done in sprint 3.

Limitations

During this thesis several limitations were encountered that affected the reliability of the results. First and foremost, the maximum speed at which a radius of curvature of 81.63 mm could be conducted as well as the maximum acceleration test on an angled surface did not produce any

relevant results. This was because the motor did not provide enough power to reach higher speeds and did not create enough torque to overcome the resistive forces on angled surfaces.

Additionally, a dummy for testing was not used in this thesis, because the motors did not have enough power to propel a mass of roughly 15 kg. This high power requirement would involve going to higher voltages and higher currents, which the lab technicians advised me not to do due to my inexperience with electrical circuits. Working with a dummy weight more closely resembles the real life situation, which would provide more accurate results. However, the results obtained are still relevant since they present a relative change in tipping frequency. This means that conclusions can still be drawn about the effectiveness of anti tipping interventions as a function of tipping probability.

Furthermore, the speed of the wheelchair at which the tests were performed was not always the same. Prior to the tests the speed was measured using a known distance. All tests were performed with this run up distance to ensure that the speed was more or less the same across the tests. However during the tests the camber of the wheels could be changed slightly, because the motor was not secured strong enough to the wheelchair frame. This caused a change in friction and thereby a change in output speed and direction.

Lastly the curb approach angles also proposed a challenge. As can be seen in figure 17b lines were drawn to mark the path for all approach angles. The wheelchair was set up along the path but was able to drift a little as a result of different output speeds for the rear wheels.

Future perspectives

For future research the use of GST and camber can be investigated as a function of tipping probability. GST is a relatively new expensive technique, but possibly holds high potential to reduce tipping probability.

Furthermore, it would be beneficial to reproduce this thesis using sensors like accelerometers to ensure that the rear wheels always have the same output speed. An encoder sensor could also be considered to achieve this. Additionally a test site with cut off approach angles could be used instead of the path lines drawn on the curbs.

Lastly, to validate the results from this thesis the tests can be done using a motor with more power. This would mean all tests could be performed with a dummy and therefore more accurate conclusions can be drawn about tipping probability.

5. Conclusion

After performing 4 sprints, testing 4 prototypes, it is evident that anti tipping wheels present the most effective method to reduce tipping probability among the proposed prototypes. Anti tipping wheels significantly enhanced rear static tipping angle by threefold and prevented tipping in dynamic tests of both curb heights. Furthermore, a heavy bottom structure proved to be beneficial in improving stability, increasing the rear and front static tipping angles by 4 degrees. Battery placement was only effective in the 50 mm curb test, but did not provide any further measurable differences in tipping probability nor did minor changes in volumetric dimensions (105% up to 110% of original dimensions). Thus combining a lowered center of mass and anti tipping wheels offers a solution to significantly reduce tipping probability and thereby enhancing user safety for a PAPAW.

Future research should focus on refining the proposed designs and exploring advanced stabilization technologies, such as a gyroscopic stabilization system to improve wheelchair stability and user safety.

6. References

[1] Pousada García, T., Groba González, B., Nieto Rivero, L., Pereira Loureiro, J., Díez Villoria, E., & Pazos Sierra, A. (2015). "Exploring the Psychosocial Impact of Wheelchair and Contextual Factors on Quality of Life of People with Neuromuscular Disorders." *Assistive technology : the official journal of RESNA*, *27*(4), 246–256. https://doi.org/10.1080/10400435.2015.1045996

[2] Gilani, R. "How many wheelchair users in the world?" *Gilani Mobility*. Mar . 1, 2024. Available: https://www.gilanimobility.ae/how-many-wheelchair-users-in-the-world/#:~:text=How%20Many%20People%20Uses%20Wheelchairs,are%20dealing%20with%20a%20disability.

[3] Grgic J. (2022). "Use It or Lose It? A Meta-Analysis on the Effects of Resistance Training Cessation (Detraining) on Muscle Size in Older Adults." *International journal of environmental research and public health*, *19*(21), 14048. https://doi.org/10.3390/ijerph192114048

[4] Khalili, M., Kryt, G., Mortenson, W. B., Van Der Loos, H. F. M., & Borisoff, J. F. (2021). "Comparison of Manual Wheelchair and Pushrim-Activated Power-Assisted Wheelchair Propulsion Characteristics during Common Over-Ground Maneuvers." *Sensors*, *21*(21), 7008. https://doi.org/10.3390/s21217008

[5] Torkia, C., Reid, D., Korner-Bitensky, N., Kairy, D., Rushton, P. W., Demers, L., & Archambault, P. S. (2015). "Power wheelchair driving challenges in the community: a users' perspective." *Disability and rehabilitation. Assistive technology*, *10*(3), 211–215. https://doi.org/10.3109/17483107.2014.898159

[6] Choi, S. W., Woo, J., Hyun, S. Y., Jang, J. H., & Choi, W. S. (2021b). "Factors associated with injury severity among users of powered mobility devices." *Clinical and Experimental Emergency Medicine*, *8*(2), 103–110. https://doi.org/10.15441/ceem.20.078

[7] MHRA, "Guidance on the stability of wheelchairs," Mar. 2004. [Online]. Available: https://unece.org/fileadmin/DAM/trans/doc/2004/wp29grsg/GRSG-ig-access-03-10.pdf

[8] Chen, W. Y., Jang, Y., Wang, J. D., Huang, W. N., Chang, C. C., Mao, H. F., & Wang, Y. H. (2011). "Wheelchair-related accidents: relationship with wheelchair-using behavior in active community wheelchair users." *Archives of physical medicine and rehabilitation*, *92*(6), 892–898. https://doi.org/10.1016/j.apmr.2011.01.008

[9] Kirby, R Lee MD; Ackroyd-Stolarz, Stacy A. BSc (OT); Brown, Murray G. PhD; Kirkland, Susan A. PhD; MacLeod, Donald A. MSc (1994). "WHEELCHAIR-RELATED ACCIDENTS CAUSED BY TIPS AND FALLS AMONG NONINSTITUTIONALIZED USERS OF MANUALLY PROPELLED WHEELCHAIRS IN NOVA SCOTIA." *American Journal of Physical Medicine & Rehabilitation. 73(5.):p 319-330.* https://journals.lww.com/ajpmr/abstract/1994/09000/wheelchair_related_accidents_caused_by_tips_and.4.aspx

[10] R. C. Hibbeler. "Engineering mechanics: Dynamics (fourteenth edition)." Hoboken, New York: Pearson Prentice Hall (2016).

[11] Winter, A., Hotchkiss, R.. "Mechanical principles of wheelchair design." *Massachusetts Institute of Technology, & Whirlwind Wheelchair International. (n.d.).* https://web.mit.edu/awinter/Public/Wheelchair/Wheelchair%20Manual-Final.pdf

[12] P. Hutterer, "It's all about Physics: Tipping - Rosenbauer Blog," *Rosenbauer Blog*, Nov. 03, 2020. [Online]. Available: https://www.rosenbauer.com/blog/en/driving-safety-tipping/

[13] Alber GmbH, "e-motion DuoDrive," 44.002.6.02.01 datasheet, May. 2021. Available: https://www.alber.nl/fileadmin/media/Downloads/NL/brochures/Alber_brochure_e-motion_DuoDrive_NL.pdf?_gl=1*ohd3cb*_up*MQ..&gclid=Cj0KCQjwlZixBhCoARIsAIC745DIGrDNrj_K7rzFNxjwOqbYMXCeaHL_HwyaCmD6kp6Emq5ZJMS99wEaAunbEALw_wcB

[14] Sunrise medical (accessed 2024), "QUICKIE Xtender Power Assist Wheelchair Accessory." *Sunrise Medical*. [Online]. Available: https://www.sunrisemedical.com/power-assist/quickie/power-assist-wheels/xtender#specifications

[15] Karmarkar, A., Cooper, R. A., Liu, H. Y., Connor, S., & Puhlman, J. (2008). "Evaluation of pushrim-activated power-assisted wheelchairs using ANSI/RESNA standards." *Archives of physical medicine and rehabilitation*, *89*(6), 1191–1198. https://doi.org/10.1016/j.apmr.2007.10.029

[16] Sonenblum, S. E., Sprigle, S., & Lopez, R. A. (2012). "Manual wheelchair use: Bouts of mobility in everyday life." *Rehabilitation Research and Practice*, *2012*, 1–7. https://doi.org/10.1155/2012/753165

[17] Digital society school, "*MoSCoW*.", The design method toolkit, (accessed 2024). [Online]. Available: https://toolkits.dss.cloud/design/method-card/moscow/

[18] Tsai, C., Lin, C., Huang, Y., Lin, P., & Su, F. (2012). "The effects of rear-wheel camber on the kinematics of upper extremity during wheelchair propulsion." *BioMedical Engineering Online,* 11(1). https://doi.org/10.1186/1475-925x-11-87

[19] A. Speight (2020). "Camber – Degrees of Performance." *Motion Composites Blog post*. https://www.motioncomposites.com/en_ca/community/blog/tips-and-tricks/camber-degrees-of-performance

[20] Veeger, D. H. E. J., Van der Woude, L. H., & Rozendal, R. H. (1989). "The effect of rear wheel camber in manual wheelchair propulsion." *J Rehabil Res Dev*, *26*(2), 37-46. https://www.rehab.research.va.gov/jour/89/26/2/pdf/Veeger.pdf

[21] Team, P. P., & Team, P. P. (2021, December 1). "What is wheelchair camber and why does it matter to you?" *Passionate People by Invacare*. https://passionatepeople.invacare.eu.com/what-is-wheelchair-camber-and-why-does-it-matter-to-you/#:~:text=Greater%20cost%3A%20Cambered%20chairs%20often,or%20to%20make%20it%20lightweight.

[22] Halliday, D., Resnick, R., & Walker, J. (2013). "Fundamentals of physics extended". *Wiley*. https://elearn.daffodilvarsity.edu.bd/pluginfile.php/987150/mod_label/intro/fundamentals-of-physics-textbook.pdf

[23] Warguła, Ł., Wieczorek, B., & Kukla, M. (2019). "The determination of the rolling resistance coefficient of objects equipped with the wheels and suspension system – results of preliminary tests." *MATEC Web of Conferences*, *254*, 01005. https://doi.org/10.1051/matecconf/201925401005

[24] E. Pavlidou, M. G. M. Kloosterman, J. H. Buurke, J. S. Rietman, and T. W. J. Janssen, "Rolling resistance and propulsion efficiency of manual and power-assisted wheelchairs," *Medical Engineering & Physics*, vol. 37, no. 11, pp. 1105–1110 (Nov. 2015). doi: 10.1016/j.medengphy.2015.08.012. https://www.sciencedirect.com/science/article/pii/S1350453315002052?via%3Dihub

[25] Dutch, B. (2020, May 12). "A huge transformation in 's-Hertogenbosch." *BICYCLE DUTCH*. https://bicycledutch.wordpress.com/2020/04/29/a-huge-transformaton-in-%CA%BCs-hertogenbosch/

[26] Migliacio M, Wong A (2017, September 13). "Using the Pmod DHB1 with Arduino Uno." *Hackster.io*. https://www.hackster.io/58089/using-the-pmod-dhb1-with-arduino-uno-70a423

[27] C. Avram and M. Măruşteri, "Normality assessment, few paradigms and use cases," *Revista Română De Medicină De Laborator*, vol. 30, no. 3, pp. 251–260, Jul. 2022, doi: 10.2478/rrlm-2022-0030.

[28] E. Ostertagová, O. Ostertag, and J. Kováč, "Methodology and application of the Kruskal-Wallis Test," *Applied Mechanics and Materials*, vol. 611, pp. 115–120, Aug. 2014, doi: 10.4028/www.scientific.net/amm.611.115.

[29] Samantha Lomuscio, "Getting Started with the Kruskal-Wallis Test | UVA Library." *University of Virginia Library* (2021, 7th of December) https://library.virginia.edu/data/articles/getting-started-with-the-kruskal-wallis-test

[30] Scipy, *scipy.stats.chi2*, "Scipy.Stats.chi2 — SciPY v1.14.0 Manual." (n. d). https://docs.scipy.org/doc/scipy/reference/generated/scipy.stats.chi2.html#scipy-stats-chi2

[31] Kirby, R. L., Thoren, F. A., Ashton, B. D., & Ackroyd-Stolarz, S. A. (1994). "Wheelchair Stability and Maneuverability: Effect of varying the horizontal and vertical position of a Rear-Antitip device." *Archives of Physical Medicine and Rehabilitation*, *75*(5), 525–534. https://doi.org/10.1016/s0003-9993(21)01614-2

[32] L. Thomas, J. Borisoff, and C. J. Sparrey (Nov. 2018). "Manual wheelchair downhill stability: an analysis of factors affecting tip probability," *Journal of Neuroengineering and Rehabilitation*, vol. 15, no. 1, doi: 10.1186/s12984-018-0450-3.

7. Appendix

Appendix A - CAD drawing

Technical drawing base structure:

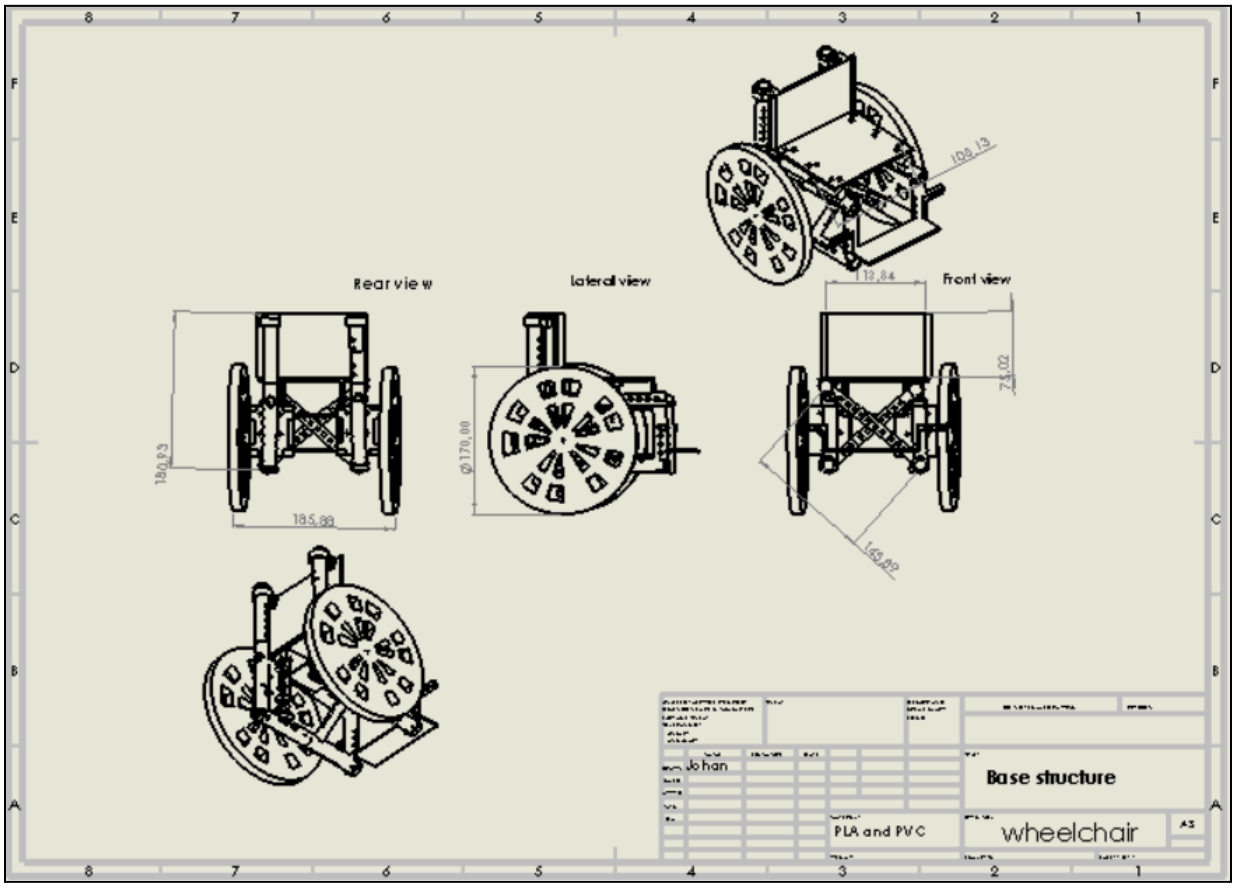

Appendix B - Arduino code

This arduino code was taken and modified from a project by Martha Miglacio and Alex Wong (2017), https://www.hackster.io/58089/using-the-pmod-dhb1-with-arduino-uno-70a423:

```
//pin connections

#define DIR1 2 //Arduino pin connected to DIR1
#define EN1  3 //Arduino pin connected to EN1
#define DIR2 8 //Arduino pin connected to DIR1
#define EN2  9 //Arduino pin connected to EN1


void setup()

{
      Serial.begin(9600); // initialization of the serial monitor
      pinMode(DIR1, OUTPUT); // Pin configuration
      pinMode(EN1, OUTPUT);
      analogWrite(EN1, 0); //stop motor
      digitalWrite(DIR1, LOW); //forward

      pinMode(DIR2, OUTPUT); // Pin configuration for Motor 2
      pinMode(EN2, OUTPUT);
      analogWrite(EN2, 0); //stop motor 2
      digitalWrite(DIR2, LOW); //forward motor 2
}


void loop()

{
      Serial.println("Enter a command (bm forward XX YY, bm backward
      (XX YY), bm stop, where xx and yy are the speed in %)");
      //indication
      while (Serial.available() == 0); // Waiting for input
      String input = Serial.readString(); // saving the command

      //parse input string for both motors at different speeds
      if (input.startsWith("bm forward")) { //check if string starts
      with "bm forward"
            Serial.println("Driving motor 1 and 2 forward"); //feedback
            for user
            analogWrite(EN1, 0); //stop motor 1
            digitalWrite(DIR1, LOW); //forward motor 1
```

```
        analogWrite(EN2, 0); //stop motor 2
        digitalWrite(DIR2, LOW); //forward motor 2

        int sp1 = getSpeed(input.substring(11,13)); //parse input
        string to get speed 1
        int sp2 = getSpeed(input.substring(14,16)); //parse input
        string to get speed 2
        analogWrite(EN1, sp1); //set that speed 1
        analogWrite(EN2, sp2); //set that speed 2
        Serial.print("Motor1 speed = ");
        Serial.print(map(sp1, 0, 255, 0, 100));  //convert from
        analogWrite input (0-255) to % and display
        Serial.println("%");
        Serial.print("Motor2 speed = ");
        Serial.print(map(sp2, 0, 255, 0, 100));  //convert from
        analogWrite input (0-255) to % and display
        Serial.println("%");
}

else if (input.startsWith("bm backward")) {  //check if string
starts with "bm backward"
        Serial.println("Driving motor 1 and 2 backward");
        analogWrite(EN1, 0); //stop motor 1
        digitalWrite(DIR1, HIGH); //backward motor 1
        analogWrite(EN2, 0); //stop motor 2
        digitalWrite(DIR2, HIGH); //backward motor 2

        int sp1 = getSpeed(input.substring(12,14)); //parse input
        string to get speed 1
        int sp2 = getSpeed(input.substring(15,17)); //parse input
        string to get speed 2
        analogWrite(EN1, sp1); //set that speed 1
        analogWrite(EN2, sp2); //set that speed 2
        Serial.print("Motor1 speed = ");
        Serial.print(map(sp1, 0, 255, 0, 100));  //convert from
        analogWrite input (0-255) to % and display
        Serial.println("%");
        Serial.print("Motor2 speed = ");
        Serial.print(map(sp2, 0, 255, 0, 100));  //convert from
        analogWrite input (0-255) to % and display
        Serial.println("%");
}

else if (input.startsWith("bm stop")) {  //check if string starts
with "bm stop"
        Serial.println("Stopping motors");
        analogWrite(EN1, 0); //stop motor 1
```

```
            analogWrite(EN2, 0); //stop motor 2
      }

      else {  //invalid command
            Serial.println("Invalid command");
      }

      Serial.println();
      delay(50); //wait a bit (0.001s)

}


//parse string to get speed

int getSpeed(String speed) {
      int sp = 0;
      sscanf(speed.c_str(), "%i", &sp); //convert string to number

      //restrain the number between 0 and 100
      if (sp < 0) {
            sp = 0;
      }

      else if (sp > 100) {
      sp = 100;
      }

      sp = map(sp, 0, 100, 0, 255); //convert percentage to value for PWM
      return sp;
}
```

Appendix C - p-value Python code

```
import scipy.stats as stats

def pval(H, df):
    return 1 - stats.chi2.cdf(H, df)

H = 18.66744
df = 3
result = pval(H, df)
print(f"CHISQ.DIST.RT({H}, {df}) = {result}")
```